

Design rules of the CMOS inverter for voltage converters

Jan Marek, Jiří Hospodka, Ondřej Šubrt

Faculty of Electrical Engineering at Czech Technical University in Prague, Technická 2,
166 27 Prague, Czech Republic

Abstract—This paper presents a description of the dominant characteristics of the CMOS inverter, which is used for voltage converters—charge pumps applications. This circuit controls transport charge between main capacitors to create a higher DC voltage. The significant part of the pump losses is caused by the inverter cross current. This current flows through the inverter in transition state and discharges the capacitor, therefore decreases the pump voltage gain. The CMOS inverter design is based on the analog block description for high-voltage integrated circuits using BSIM model equations. The main benefit of this article is derived analytical relationship between width and length of the NMOS and PMOS transistors to achieve the static power minimization. The derivation has been performed based on the sensitivity analysis. The design relationship are applicable to the other MOSFET models, as EKV. The characteristic of the proposed circuit has been verified by simulation in ELDO Spice. Analysis results show that the cross current is reduced by ten times in comparison with the value of the standard digital inverter (with symmetrical voltage transfer characteristics). This improvement was achieved while keeping relatively large area of both transistors satisfying the dynamic properties.

Index Terms—CMOS inverter, cross current, charge pump, BSIM model, high-voltage, sensitivity.

I. INTRODUCTION

A CMOS inverter is a basic block (Fig. 1) for digital design circuits which performs a logic operation from A to A. However, there are also applications in the analog domain; both continuous-time circuits (oscillators, amplifiers) and discrete-time analog circuits (voltage converters). Although discrete-time analog circuits seem to be digital circuits from a system perspective, the internal state of the system is time continuous during each period of the clock signal. Charge pumps ([6], [7], [8]) are a typical group of switched-capacitor (SC) circuits, where the inverter drives switch to a transport charge between the main capacitors. The output voltage of the inverter with a capacitive load may be in an undefined state from the view of logic levels because energy accumulated in capacitors must be a continuous function of time. Results of the transient analysis show that the dominant part of losses in charge pumps is caused by a DC cross current that flows through an inverter operating in the linear region of voltage transfer characteristics. This is undesirable because the cross current greatly decreases a pump's voltage gain while losses caused by propagation delays of the inverter are very small.

Current research deals with the dynamic behavior of the inverter and transistor sizing, which is based on the equivalent digital model. A number of detailed analyses in

digital circuits ([1], [4], [12]–[19]) have been reported ([15]–[19]). The inverter operating in a strong inversion is known. The width of the PMOS must be 2-3 times width of the NMOS [1] (symmetrical transfer characteristics). However, this setting may not suit in analog circuits.

In the article, the inverter design for voltage converters is discussed in order to minimize the average cross current during the period of the clock signal. Using BSIM model equations, an analytical description of DC characteristics ([1], [4]) will be found for this purpose. The strong inversion region is expected in the high-voltage circuits, where the behavior of the MOSFET models for analog structured design is correct. Consequently, it is not necessary to admit a specified technology, because the EKV parameters are extracted from the curves simulated using the BSIM models [3]. The main benefit of this article is an analytical relationship between sizing (width and length) of both the transistors to achieve the static power minimization of the charge pump inverter. The acquired estimation can be used as the baseline for the optimizing algorithm.

II. BSIM MODEL EQUATION

A real model of the MOSFET, like BSIM involves many effects [2]. It contains many model parameters and any derivation is very difficult (implicit form, solving of irrational equations, etc.). So, the equations are simplified to only describe the dominant characteristics for the design purpose. The static model of MOSFET is discussed as introduced in the previous text.

For MOSFET operation in high-voltage circuits where $V_{GS} \ll V_{TH}$, the following conditions must be true:

- long channel MOSFET
- strong inversion region.

Channel length is an important parameter because of the breakdown voltage. The electrical field in a structure induced by an applied voltage must be significantly less than the critical electrical field, $E = \frac{V}{L_{eff}} \leq E_{crit}$, where L_{eff} is effective channel length. A critical electrical field is limited to the value given by a semi-empiric model [2].

The effective channel length is relative to the applied voltage V_{max} (gate-source, drain-source) defined as

$$L_{eff} \gg V_{max} \frac{\mu_{eff}}{2v_{sat}}, \quad (1)$$

where v_{sat} is the saturation velocity (model parameter) and μ_{eff} is effective mobility.

A drain current model is given by a single equation [2]. The transition from triode to the saturation region is ensured through an effective drain-source voltage.

$$V_{DSeff} = \begin{cases} V_{DS}, & \text{for triode region} \\ V_{DSsat}, & \text{for saturation region} \end{cases} \quad (2)$$

and for long channel MOSFETs, the saturation drain current $V_{DS} = V_{DSsat}$ is given by:

$$(3) \quad I_{Dsat0} = \frac{1}{2} \frac{W}{L} C_{oxe} \mu_{eff} V_{DSsat} (V_{GS} - V_{TH}),$$

where C_{oxe} is the electrical oxide capacitance. The boundary between the triode and saturation regions is predicted by the voltage $(V_{GS} - V_{TH})$ and applies a bias voltage effect and further model parameters (channel length and width...) included in the bulk-charge equation [2], labeled A_{bulk} . A_{bulk} is closed to unity for relatively high source-bulk bias voltage. In the other words,

$$V_{DSsat} = \frac{V_{GS} - V_{TH}}{A_{bulk}} \approx V_{GS} - V_{TH} \text{ for } V_{SB} > V_{GS}. \quad (4)$$

Generally, the output I-V curve in the saturation region ($V_{DS} > V_{DSsat}$) is written by several physical mechanisms. Nevertheless, considering the condition (1) short channel effect- channel length modulation (CLM) and Substrate Current Induced Body Effect (SCBE) can be neglected. Then the drain current increases linearly with the V_{DS} voltage. The slope of the output characteristics is mainly determined by Early voltage V_{ADIBL} due to the drain-induced barrier lowering (DIBL) effect ([1], [2], [5]). V_{ADIBL} is directly proportional to the voltage V_{GS} , as is shown below. Moreover, the equation (5) contains the model parameters PDIBLC2 and PDIBLCB [2].

$$V_{ADIBL} = \frac{1}{2} \frac{V_{GS} - V_{TH}}{PDIBLC2 (1 - PDIBLCB V_{SB})} \quad (5)$$

The complex drain current equation may be expressed by the formula

$$I_{Dsat} = I_{Dsat0} \left(1 + \frac{V_{DS} - V_{DSsat}}{V_{ADIBL}} \right)$$

for $V_{DS} \geq V_{DSsat}$.

The drain current in the triode region is a function of the V_{DS} voltage ($V_{GS} = \text{const.}$). The maximum of the parabolic function $I_{DS0} = f(V_{DS})$ corresponds to the voltage V_{DSsat} because of the neglected CLM mechanism ([1], [2], [5]). Then, the relationship between the drain-source voltage V_{DS} and the saturation drain current I_{Dsat0} [5] can be written simply as

$$I_{DS0}(V_{DS}) = -\frac{I_{Dsat0}}{V_{DSsat}^2} V_{DS}^2 + \frac{I_{Dsat0}}{V_{DSsat}} 2V_{DS}$$

for $V_{DS} < V_{DSsat}$.

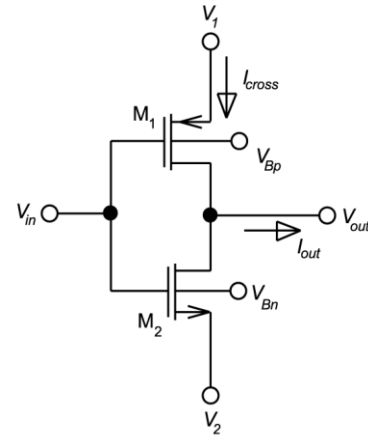


Fig. 1. The CMOS inverter.

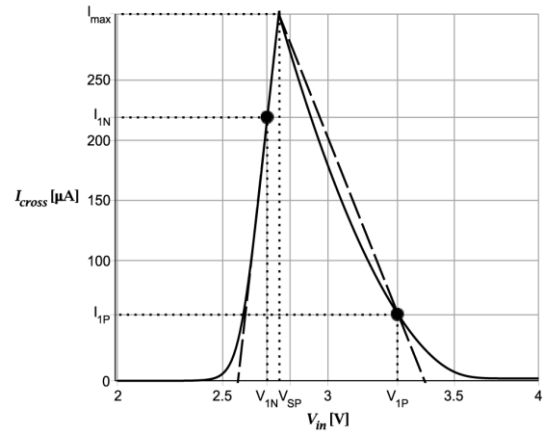


Fig. 2. DC current characteristics of the inverter.

III. STATIC PARAMETERS OF THE CMOS INVERTER

A diagram of the CMOS inverter schematic is shown in Fig. 1. All voltages are referenced to the ground and $V_1 - V_2 > V_{THN} + |V_{THP}|$.

The inverter's cross current characteristics is shown in Fig. 2. A general form of the analytical expression of the cross current is divided into the three cases:

$$I_{cross} = \begin{cases} I_{DsatN} | V_{GS} = V_{in} - V_2, & \text{for C1} \\ I_{DsatP} | V_{SG} = V_1 - V_{in}, & \text{for C2} \\ 0, & \text{otherwise,} \end{cases} \quad (8)$$

where condition C1 is: $V_2 + V_{THN} \leq V_{in} \leq V_{SP}$ and C2 is: $V_{SP} \leq V_{in} \leq V_1 - |V_{THP}|$.

Cross current is maximal at the switching point $V_{in} = V_{SP}$, see [1]. Both transistors M_1 and M_2 are in the saturation region (Eq. 6) for this case and the drain current of each MOSFET must be equal:

$$I_{DsatN} | V_{GS} = V_{SP} - V_2 = I_{DsatP} | V_{SG} = V_1 - V_{SP}, \quad (9)$$

if the output current (see Fig. 1) is zero ($I_{out} = 0$). Equation (9) is more than third order for variable V_{SP} , thus simplifying preconditions will be introduced.

Firstly, Early voltage (Eq. 5) limits to infinity, wherefrom it is compared $I_{Dsat0N} \approx I_{Dsat0P}$. Secondly, the absolutely value of the drain currents of the PMOS and NMOS transistors for the derivation V_{SP} are not important; only transconductance is important. The slope of the cross current characteristics on each interval is mainly given by the linear part of the voltage $V_{GS} - V_{TH}(V_{SB})$ (MOS transconductance in strong inversion is a linear function of the gate-source voltage), while other powers at that voltage are not taken into account. Hence, the bulk charge equation [2] is adjusted to

$$A_{bulk0}(V_{SB}) = A_{bulk}(V_{GS} - V_{TH})_{eff=0}$$

and with the effective mobility substituted into the equation (3) at zero bias voltages. Finally, the formula of the switching point for the BSIM model [1] can be expressed in the modified form:

$$V_{SP} = \frac{V_1 - |V_{THP}(V_{BS})| + \sqrt{R \frac{a}{b}} [V_2 + V_{THN}(V_{SB})]}{1 + \sqrt{R \frac{a}{b}}}, \quad (10)$$

where $a = \frac{C_{oxeN} \mu_{effN} |V_{GS} - V_{SB}|}{A_{bulk0N} |V_{SB}=0}$, $b = \frac{C_{oxeP} \mu_{effP} |V_{SG} - V_{BS}|}{A_{bulk0P} |V_{BS}=0}$ and $R = \frac{W_n L_p}{L_n W_p}$.

The switching point is an important parameter for the calculation of DC power because of the discontinuous cross current characteristics at that point, as it is shown in Fig. 2. The typical characteristics of the dependence of the switching point on the ratio dimensions of both transistors is shown in Fig. 3.

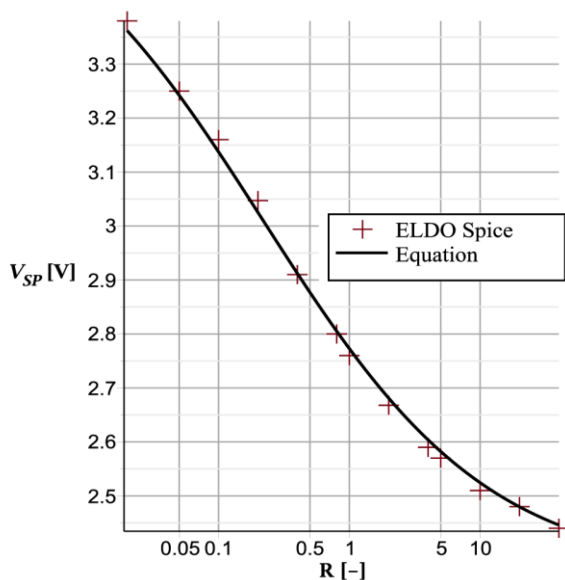


Fig. 3. Switching point analysis – dependence on the ratio R

Static power during the inverter's output voltage crossing between logic 1 and logic 0 is defined as

$$P_{DC} = \int_{V_2}^{V_1} I_{cross}(V_{in}) dV_{in} = \int_{V_2+V_{THN}}^{V_{SP}} I_{DsatN}(V_{in}) dV_{in} + \int_{V_1-|V_{THP}|}^{V_{SP}} I_{DsatP}(V_{in}) dV_{in}. \quad (11)$$

The solution of equation (11) exists, but it is confusing and unnecessary for the estimation of the power dissipation. Results of the numeric integration of equation (11) shows that function is primarily determined by the function \arctan^1 , that can be approximated by its argument (linear function) at zero $\lim_{x \rightarrow 0} \left(\frac{\arctan(x)}{x} \right) = 0$. A simpler approach is based on an approximation of the characteristics (Fig. 1) in intervals $V_{in} \in (V_2 + V_{THN}, V_{SP})$ and $V_{in} \in (V_{SP}, V_1 + |V_{THP}|)$ by linear interpolation for two points at each interval:

- At the point corresponding to the known voltage V_{SP} that is substituted into equation (5):

$$I_{max}|_{V_{in}=V_{SP}} = I_{DsatN}|_{V_{GS}=V_{SP}-V_2} \approx I_{DsatP}|_{V_{SG}=V_1-V_{SP}}$$

At the point where $|V_{GS}|$ is greater than the threshold voltage $|V_{TH}|$ (strong inversion region), the transistor is operating at the edge of the saturation region (M_1 for $V_{in} \in (V_{SP}, V_1 + |V_{THP}|)$ and M_2 for $V_{in} \in (V_2 + V_{THN}, V_{SP})$), where the drain current is approximately the linear function of the gate-source voltage. It means that quadratic part of $V_{GS} - V_{TH}$ must be less than its linear part. Assuming the equality of these parts, two solutions exist. The first one is $V_{GS} = 0$ that is ignored and the second is $V_{GS} = 2|V_{TH}|^2$:

$$I_1 = \begin{cases} I_{1N} = I_{Dsat0N}|_{V_{GS}=V_{1N}=2V_{THN}}, & \text{for NMOS} \\ I_{1P} = I_{Dsat0P}|_{V_{SG}=V_{1P}=2|V_{THP}|}, & \text{for PMOS} \end{cases}$$

then, new formula for cross current characteristics can be expressed as

$$\tilde{I}_{cross} \approx \begin{cases} I_{1N} \frac{V_{SP}-V_{in}}{V_{SP}-V_2-2V_{THN}} + I_{max} \frac{V_2+2V_{THN}-V_{in}}{V_2+2V_{THN}-V_{SP}}, & \text{for C1} \\ I_{1P} \frac{V_{SP}-V_{in}}{V_{SP}-V_1+2|V_{THP}|} + I_{max} \frac{V_1-2|V_{THP}|-V_{in}}{V_1-2|V_{THP}|-V_{SP}}, & \text{for C2} \\ 0, & \text{otherwise,} \end{cases} \quad (12)$$

where condition C1 is: $V_2 + V_{THN} \leq V_{in} \leq V_{SP}$ and C2 is: $V_{SP} < V_{in} \leq V_1 - |V_{THP}|$. The equation (12) allows to calculate the static power as the triangle area:

$$\tilde{P}_{DC} \approx \frac{1}{2} I_{max} \left(\frac{I_{max}(V_1 - 2|V_{THP}|) - I_{1P}V_{SP}}{I_{max} - I_{1P}} - \frac{I_{max}(V_2 + 2V_{THN}) - I_{1N}V_{SP}}{I_{max} - I_{1N}} \right). \quad (13)$$

¹Analytical expression is given by the sum of the functions \arctan and \ln .
²This value is also included in the coefficient at the \arctan in the solution of Eq. (11).

The average current during the transition between both the logic levels is the coinciding DC power divided by the power supply voltage:

$$I_{av} = \frac{P_{DC}}{V_1 - V_2}. \quad (14)$$

IV. STATIC POWER MINIMIZATION

Static power dissipation dependence on the dimensions of both transistors M_1 and M_2 is discussed in this section. Static power is reduced by reducing an inverter's peak current (Fig.2) $I_{max} = f(V_{SP})$. Implying that, the switching point should be closed to voltage $V_2 + V_{THN}$ (lower limit) or $V_1 - |V_{THP}|$ (upper limit) to turn off one of either transistor (equation 13). However, this state cannot really be obtained because $R \rightarrow 0$ for the lower limit or $R \rightarrow \infty$ for the upper limit (Fig. 3), as it is shown in Fig. 3. The setting of the optimal ratio R to effective reduction of static power can be found by the sensitivity analysis of the switching point to the parameter R (Eq. 10). The sensitivity is defined as

$$C = \frac{dV_{SP}}{dR} \frac{R}{V_{SP}} = -\frac{1}{2} \frac{aR(V_1 - |V_{THP}| - V_2 - V_{THN})}{\left(\sqrt{\frac{aR}{b}} + 1\right) \sqrt{\frac{aR}{b}} b} \quad (15)$$

and decrease of the maximum sensitivity to the desired value is expressed by parameter δ :

$$\delta = \frac{C_{opt}}{C_{max}} \quad (16)$$

The δ parameter will be determined by the simulation results as it is shown below. δ is usually put to 0.5 because the voltage V_{SP} depends on the square root of R . Maximum sensitivity (in absolute value) given by the condition $\frac{dC}{dR} = 0$ is at the point

$$R_{Cmax}|_{C=C_{max}} = \frac{V_1 - |V_{THP}|}{\frac{a}{b}(V_2 + V_{THN})} \quad (17)$$

The normalized sensitivity curve to the maximum absolute value is shown in Fig. 4.

Finally, the optimal parameter R is derived from equations (15), (16) and (17),

$$R_{opt} = \frac{1}{16} \left[\frac{2C_{max}\delta(V_{1a} + V_{2a}) + V_{12} \pm \sqrt{V_{12}^2 + 4C_{max}\delta(V_{1a} + V_{2a} + C_{max}V_{12}\delta) + V_{12}}}{\sqrt{\frac{a}{b}} C_{max}\delta V_{2a}} \right]^2 \quad (18)$$

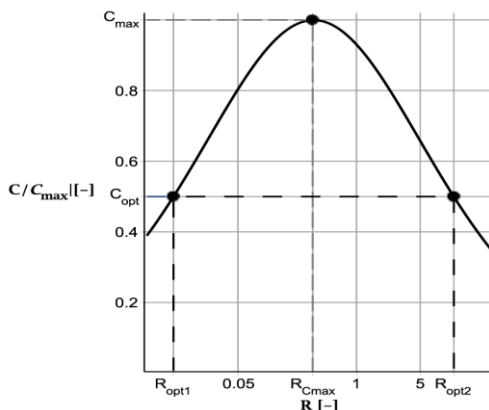


Fig. 4. Normalized sensitivity curve

where $V_{1a} = V_1 - |V_{THP}|$, $V_{2a} = V_2 + V_{THN}$ and $V_{12} = V_{1a} - V_{2a}$. Two solutions for the equation (18) exist. The first: R_{opt1} for $\frac{W_n}{L_n} \gg \frac{W_p}{L_p}$ and the second: R_{opt2} for $\frac{W_p}{L_p} \gg \frac{W_n}{L_n}$ (Fig. 3). The calculated ratio R dependence on the chosen parameter δ is shown in Tab. II.

V. SIMULATION RESULTS

The DC parameters of the CMOS inverter were simulated by ELDO. The simulation circuit parameters are shown in Tab. I. The dependence of the average cross current (Eq. 14) on the width of the PMOS (W_p) or NMOS (W_n) transistor was analyzed at the fixed channel lengths L_n, L_p . These were determined based on the condition (1), respecting the value of the bias voltages, as it is shown in Table I.

TABLE I: SIMULATION CIRCUIT PARAMETERS

	Parameter	Value
Power supply voltages	V_1 V_2	4 V 2 V
Threshold voltage of the N/PMOS	V_{THN} $ V_{THP} $	0.356 V 0.33 V
Coefficients calculated from Eq.10	a b	$3.43 \cdot 10^{-4} \text{ AV}^{-2}$ $7.45 \cdot 10^{-5} \text{ AV}^{-2}$

Analysis results in Tab. II show that an effective reduction of I_{av} is achieved when $R \gg R_{Cmax}$ (solution R_{opt1} of Eq. 18), consequently $W_n \gg W_p$ and V_{SP} approach the lower limit, $V_{SP} \rightarrow V_2 + V_{THN}$. This is physically caused by a greater mobility of electrons in the NMOS structure compared to the mobility of holes in the NMOS dimensions. Otherwise, when $R \ll R_{Cmax}$, a very large disproportion between sizes of both transistors adversely affects other properties of the inverter (transistors area, dynamic properties,...), as is shown below. Of course, the mean value of the cross current is not only a function of R , but depends on the specific value of $W_n/L_n, W_p/L_p$ respectively, as is shown in Fig. 5. These specific sizes of the NMOS and PMOS transistors can be set by additional application requirements (time delay, switching characteristics), but the ratio R must be retained. Experience says that the optimal value of the parameter δ is $0.4 \div 0.6$ (Eq. 16) for practical design. Values of the ratio R and the average cross current I_{av} for this range of the δ parameter are bold in Tab. II.

TABLE II: SIMULATION RESULTS

Channel length of the N/PMOS: $L_p = L_n = 1 \mu\text{m}$				
δ	Width of the N/PMOS:		I_{av} [mA]	
	$R_{opt1,2}[-]$	V_{SP} [V]	$W_n = 40 \mu\text{m}$	$W_p = 40 \mu\text{m}$
0.51	0.01	3.47	1.92	0.018
0.63	0.02	3.4	1.69	0.031
0.92	0.1	3.16	1.07	0.106
0.985	0.2	3.047	0.798	0.159
1	0.34	2.76	0.309	0.309
0.83	2	2.67	0.186	0.372
0.7	4	2.59	0.107	0.430
0.66	5	2.57	0.089	0.447
0.5	11.7	2.5	0.047	0.507
0.41	20	2.46	0.026	0.541
0.31	40	2.42	0.013	0.582

However, the optimal setting of R may not be optimal for the design of an inverter operating in digital circuits, where

the switching point (Eq. 10) should be closed to the ideal value of half of the supply voltage. Therefore

$$R|_{V_{SP}=V_{DD}/2} = \frac{b}{a} \left[\frac{V_1 - V_2 - 2|V_{THP}(V_{BS})|}{V_1 - V_2 - 2V_{THN}(V_{SB})} \right]^2 \quad (19)$$

and corresponding sensitivity is about 0.98 and simulated I_{av} value is about ten times higher compared to the optimization process. The width of the PMOS transistor is sized to 2 ÷ 3 the width of the PMOS [1] transistor (lengths are the same), provided that $V_{THN} \approx |V_{THP}|$. This condition can not be satisfied in voltage converters due to a different supply voltage V_1, V_2 in each of the converter's stages and the different threshold voltage of each of the transistors (body effect, [1]–[5]).

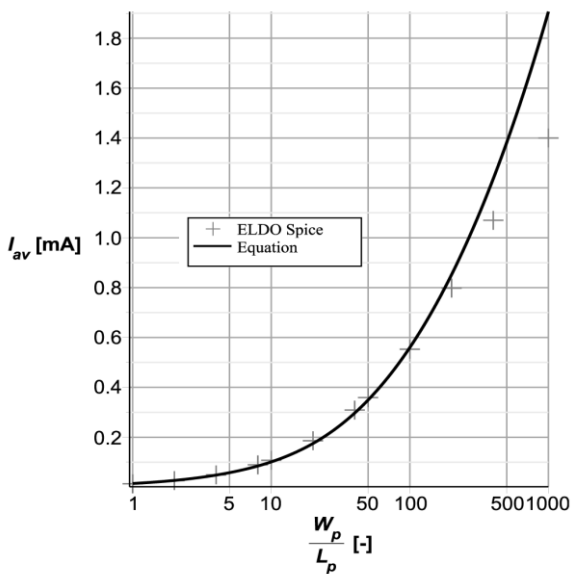


Fig. 5. Cross current vs. the W_p/L_p ratio

VI. CONCLUSION

The inverter draft for charge pump applications as an analog block is discussed in this paper. Design process via the symbolic description is based on the low cross current (Eq. 8) during the transition between logic high and logic low levels. The sensitivity analysis of the switching point to the sizing of the transistors (Fig. 4) shows that it is possible to find the optimal ratio $R = \frac{W_n L_p}{L_n W_p}$, while keeping a relatively big ratio W/L value of each of the NMOS and PMOS transistors. It is very favorable from a time response perspective. The formulae derived in this paper are applicable to the other MOSFET models including the parameters for the specified technology process. Important implications of the optimization process can be summarized in the following items:

- Asymmetric DC characteristics; switching point is not equal to the half supply voltage. It is not an appropriate configuration in a digital circuit (rise time versus fall time, noise margin for high versus low logic level,...), while these properties are not meaningful in analog circuits. This fact has not been solved yet.

- Propagation delays between logic levels should be short because of the possibility of setting small effective switching resistances (large width) of the NMOS and PMOS. Propagation delays are not the same.
- The cross current is very small if the operating point of the inverter is set to the linear region of the voltage transfer characteristics in comparison with cross current of the "symmetrical" inverter of the same area.
- Static and dynamic properties are insensitive to the dimensional tolerance of the transistors. The sensitivity of the proposed inverter switching point to the transistor sizing is always less than sensitivity of the inverter for digital circuit applications. It follows from the principle of the design process.

All proposals were validated by the real circuit simulations.

Charge pumps are systems that are usually designed via the simulation because of its properties taken from both digital and analog circuits (Discrete-time analog circuits). Testing and many iterations mean long-time simulation process. Thus, the analytical results will be very useful for the prediction of the required static and dynamic properties of these circuits (output voltage, rise time, etc.) without optimization process.

ACKNOWLEDGMENT

This work has been supported by the grant No. SGS14/191/OHK3/3T/13 of the CTU in Prague.

REFERENCES

- [1] R. Baker, CMOS: circuit design, layout, and simulation. 3rd ed. Hoboken, NJ: Wiley, 2010, xxxiii, ISBN 9780470881323.
- [2] C. Hu, A. M. Nikenjad, W. Yang, D. Lu, BSIM4.6.4 MOSFET Model: User's Manual. UC Berkeley, 2009.
- [3] D. Stefanović, M. Kayl, Structured analog CMOS design. Dordrecht: Springer, 2008. ISBN 9781402085727.
- [4] C. Jager, Richard C. Travis N, Microelectronic circuit design. 3rd ed. Boston: McGraw-Hill, 2008. ISBN 9780073309484.
- [5] Y. Tsividis, C. McAndrew, Operation and modeling of the MOS transistor. 3rd ed. New York: Oxford University Press, 2011, xxiv, 723 p. ISBN 0195170156.
- [6] Z. Hui, H. Mengshu, Z. Yimeng, T. Yoshihara, A 4-phase cross-coupled charge pump with charge sharing clock scheme. Electronic Devices, Systems and Applications (ICEDSA), 2011, p. 73-76.
- [7] F. Pan and T. Samaddar, Charge pump circuit design. McGraw-Hill, c2006, xv, 247 p. ISBN 978-007-1470-452.
- [8] M.-S. Shiau, Z.-H. Hsieh, C.-C. Hsieh, H.-Y. Liu, D.-G. Liu, A Novel Static CTS Charge Pump with Voltage Level Controller for DC-DC Converters. 2007 IEEE Conference on Electron Devices and Solid-State Circuits. IEEE, 2007, p. 481-484.
- [9] L. Bisdounis, S. Nikolaidis, O. Loufopavlou, Propagation delay and short-circuit power dissipation modeling of the CMOS inverter. Circuits and Systems I: Fundamental Theory and Applications, IEEE Transactions on, 1998, Vol. 45, Issue 3, p. 259-270.
- [10] B. J. Cheek, N. Stutzke, S. Kumar, J. Baker, A. J. Moll, W. B. Knowlton, Investigation of circuit-level oxide degradation and

its effect on CMOS inverter operation and MOSFET characteristics. Reliability Physics Symposium Proceedings, 2004, p. 110-116.

low-power low-voltage techniques and novel design and verification methods of data converters.

- [11] M. Hafed, M. Oulmane, N. C. Rumin, Delay and current estimation in a CMOS inverter with an RC load. Computer-Aided Design of Integrated Circuits and Systems, 2001 IEEE Transactions on. Vol. 20, Issue 1, 2001, p. 80-89.
- [12] B. G. Gawalwad, S.N. Sharma, Noise analysis of a CMOS inverter using the Itô stochastic differential equation. 2012 IEEE International Conference on, 2012, p. 344-349.
- [13] F.S. Marranghello, A.I. Reis, R.P. Ribas, CMOS inverter delay model based on DC transfer curve for slow input, Quality Electronic Design (ISQED), 2013, p. 651-657.
- [14] K. Matsumoto, T. Hirose, Y. Osaki, N. Kuroki, M. Numa, Switching voltage detection and compensation circuits for ultra-low-voltage CMOS inverters. Circuits and Systems. MWSCAS '09. 52nd IEEE International Midwest Symposium on, 2009, p. 483-486.
- [15] A.S. Chakraborty, M. Chanda, C.K. Sarkar, Analysis of noise margin of CMOS inverter in sub-threshold regime. Engineering and Systems (SCES), 2013, p. 1-5.
- [16] P. Chaourani, I. Messaris, N. Fasarakis, M. Ntogramatzi, S. Goudos, S. Nikolaidis, An analytical model for the CMOS inverter. Power and Timing Modeling, Optimization and Simulation (PATMOS), 2014, p. 1-6.
- [17] A.A. Hamoui, N.C. Rumin, An analytical current, delay, and power model for the submicron CMOS inverter. Electronics, Circuits and Systems, 1999, p. 1547-1551.
- [18] X. Peng, P. Abshire, Stochastic Behavior of a CMOS Inverter. Electronics, Circuits and Systems, 2007, p. 94-97.
- [19] A. Ruangphanit, K. Kiddee, A. Poyai, Y. Wongprasert, S. Niemcharoen, R. Muanghlua, The effects of temperature and device dimension of MOSFETs on the DC characteristics of CMOS inverter. Electrical Engineering/Electronics, Computer, Telecommunications and Information Technology (ECTI-CON), 2012, p. 1-4.

AUTHOR BIOGRAPHY

Jan Marek was born in Prague on April 8, 1990. He graduated from the Czech Technical University in Prague in 2014 and is currently studying towards Ph.D. at the Department of Circuit Theory. His research interests deal with the design of modern analog circuits, as well as their optimization.

Jiří Hospodka was born in 1967. He received his Master's and Ph.D. degrees from the Czech Technical University in Prague in 1991 and 1995, respectively. Since 2007 he has been working as associate professor at the Department of Circuit Theory at the same university. Research interests: circuit theory, analogue electronics, filter design, switched-capacitor, and switched-current circuits.

Ondřej Šubrt was born in Hradec Králové on February 24, 1977. He works as analog design engineer with ASICentrum Prague, a company of the Swatch Group. At present, he has also been appointed an Ass. Prof. at the Faculty of Electrical Engineering, CTU Prague. His research interests being analog and mixed-signal integrated circuits design with emphasis